Biochemical and Biophysical Research Communications **282,** 131–141 (2001)
doi:10.1006/bbrc.2001.4462, available online at http://www.idealibrary.com on IDEAL®

Identification and Structure of the Nerve Growth Factor Binding Site on TrkA

Alan G. S. Robertson,*[,1] Mark J. Banfield,† Shelley J. Allen,* Julie A. Dando,† Grant G. F. Mason,* Sue J. Tyler,* Gavin S. Bennett,‡ Susan D. Brain,‡ Anthony R. Clarke,† Ruth L. Naylor,* Gordon K. Wilcock,§ R. Leo Brady,† and David Dawbarn*

**Molecular Neurobiology Unit (Care of the Elderly), URCN, Bristol Royal Infirmary, Bristol BS2 8HW, United Kingdom; ‡Pharmacology Group and Vascular Biology Research Centre, Division of Biomedical Sciences, King's College, Manresa Road, London SW3 6LX, United Kingdom; †Department of Biochemistry, School of Medical Sciences, University of Bristol, Bristol BS8 1TD, United Kingdom; and §Department of Care of the Elderly, Frenchay Hospital, Frenchay BS16 1LE, United Kingdom*

Received January 29, 2001

Nerve growth factor (NGF) is involved in the development and maintenance of the nervous system and has been implicated as a possible therapeutic target molecule in a number of neurodegenerative diseases, especially Alzheimer's disease. NGF binds with high affinity to the extracellular region of a tyrosine kinase receptor, TrkA, which comprises three leucine-rich motifs (LRMs), flanked by two cysteine-rich clusters, followed by two immunoglobulin-like (Ig-like) domains. We have expressed the second Ig-like domain as a recombinant protein in *E. coli* and demonstrate that NGF binds to this domain with similar affinity to the native receptor. This domain ($TrkAIg_2$) has the ability to sequester NGF *in vitro*, preventing NGF-induced neurite outgrowth, and *in vivo*, inhibiting NGF-induced plasma extravasation. We also present the three-dimensional structure of the $TrkAIg_2$ domain in a new crystal form, refined to 2.0 Å resolution.

Key Words: **NGF/TrkA; binding domain; X-ray structure; Alzheimer's disease,**

Nerve growth factor (NGF) is one of a family of neurotrophins involved in the development and maintenance of the peripheral and central nervous systems. The other members include brain-derived neurotrophic factor (BDNF), neurotrophin-3 (NT-3) and NT-4. All the neurotrophins bind to a common receptor $p75^{NGFR}$ (1). Each neurotrophin also binds to one of a homologous family of tyrosine kinase receptors: NGF binds to TrkA (2), BDNF and NT-4/5 bind to TrkB (3, 4) and NT-3 binds to TrkC (5). NT-3 can also bind TrkA and TrkB with reduced affinity (6).

Although the overall three dimensional structure of the TrkA extracellular region is unknown, distinct structural motifs in the sequence have been characterised (7). The Trk extracellular domain comprises three tandem leucine rich motifs (LRM), flanked by two cysteine cluster regions, followed by two immunoglobulin-like (Ig-like) domains. The three-dimensional structure of the second Ig-like domain, $TrkAIg_2$, has recently been determined to 2.5 Å resolution in tetragonal space group $P4_12_12$. The structures of the equivalent domains in TrkB and TrkC were also presented (8). However, all of these structures are strand-swapped dimers in which the N-terminal A-strand of each molecule is replaced by the equivalent strand of a symmetry-related mate. In this form, none of these Ig-like domains bound their respective neurotrophin ligands. $TrkAIg_2$ also adopts a monomeric fold, and it is this form which is present in the crystal structure of the $TrkAIg_2$-NGF complex (9). In this study, a complex was firstly formed between $TrkAIg_{1,2}$ and NGF. However, over the time it took for the crystals to appear, the $TrkAIg_{1,2}$ had been proteolysed to separate $TrkAIg_1$ from $TrkAIg_2$, and the resulting crystals contained a complex consisting of a homodimer of NGF and two copies of $TrkAIg_2$. Although this complex clearly demonstrates the surfaces of $TrkAIg_2$ that interact with the neurotrophin, from the observed association it is unclear whether this domain of TrkA alone accounts for all of its contacts with its ligand.

This uncertainty is supported by a range of studies that have implicated a variety of Trk receptor surfaces in interactions with the neurotrophins. Data from Windisch *et al.* (10–12) suggested that the second LRM is responsible for NGF binding, whereas other studies

[1] To whom correspondence should be addressed. Fax: 0117 928 3137. E-mail alan.robertson@bristol.ac.uk.

0006-291X/01 $35.00

confirm the observations from the crystal structure that the Ig-like domains of the Trk receptors are central to ligand binding and receptor activation. By creating chimeric Trk receptors, swapping different TrkA domains for those on either TrkB or TrkC, Pérez *et al.* (13) concluded that both of the Ig-like domains are important for the binding of NGF to TrkA. Similar work done by Urfer *et al.* (14) indicated that the second Ig-like domain closest to the transmembrane-spanning region ($TrkAIg_2$) provides the main contacts for specific neurotrophin binding, as observed in the crystal structure. Indeed, expression of a TrkC receptor consisting of only the second Ig-like domain and the tyrosine kinase domain, was sufficient for NT3 induced autophosphorylation. We have previously reported expression of recombinant $TrkAIg_{1,2}$ consisting of both the Ig-like domains of TrkA. This protein was sufficient to bind NGF with a similar affinity to that of TrkA expressed on cells, could inhibit NGF induced neurite outgrowth of PC12 cells (rat pheochromocytoma cells) and NGF induced plasma extravasation *in vivo* (15).

To further clarify the regions of TrkA responsible for its interactions with NGF, in this study we report a comparative analysis of NGF binding to truncated forms of the TrkA receptor. In addition to the $TrkAIg_{1,2}$ construct we have previously described, we have now also produced a further truncated form which consists of amino acids 285–413, encompassing only the second Ig-like domain of TrkA ($TrkAIg_2$, previously defined as 253–375), and the region that links $TrkAIg_2$ to the membrane. These studies confirm that the second Ig-like domain is the major contributor to NGF binding, and that single-domain recombinant forms of TrkA are capable of binding NGF with high affinity and inhibiting the biological activity of NGF *in vitro* and *in vivo*. These results support the feasibility of exploiting single-domain truncated forms of TrkA as therapeutics functionally capable of sequestering NGF and evoking biological responses. In addition, we have also determined the three dimensional crystal structure of this $TrkAIg_2$ construct to 2.0 Å resolution. Although this truncated form of $TrkAIg_2$ crystallises in a different space group to the structures previously reported for similar domains from TrkA, TrkB and TrkC, it also forms strand-swapped dimers. This is surprising as the recombinant form prepared in this study, unlike those described previously, binds NGF with high affinity. As the neurotrophin binding surface is occluded in the dimer. These data indicate $TrkAIg_2$ is capable of dynamic transitions between active monomer and inactive dimeric forms. Although it is unclear whether this propensity to form strand-swapped dimers is maintained in the full-length receptor, transitions of this kind illustrate a potential mechanism for molecular switching between active and inactive forms of surface receptors.

MATERIALS AND METHODS

Cloning, expression, refolding, and purification of the Ig-like domains. As the design of these constructs preceded availability of the truncated TrkA crystal structures, assignment of the Ig-like domain boundaries utilised the PredictProtein software (16) and method described previously (15). The $TrkAIg_{1,2}$ protein was cloned and expressed as described (15). The PCR product of pET15b-$TrkAIg_{1,2}$ amplified with primers oligo10693 (CCGATCTCGAGTTATCATTCGTCCTTCTTCTCCACCGGGTC) and oligo66816 (ATCATATGCCGGCCAGTGTGCAGCT) was cloned into pET15b resulting in pET15b-$TrkAIg_2$. $TrkAIg_2$ was expressed in *E. coli* BL21 cells transformed with the above plasmid as previously described (15). This construct comprises residues 253–375 of the mature protein, and additionally has a further 21 residues at the NH2-terminus which constitute the histidine expression tag and associated thrombin cleavage sequence.

The harvested cells were resuspended in 10% glycerol, frozen at −70°C and the pellet was passed 3 times through a XPress. The extract was then centrifuged at 10,000 rpm, 4°C for 30 min to pellet the insoluble inclusion bodies. The inclusion bodies were then washed in 500 ml 1% (v/v) Triton X-100, 10 mM Tris–HCl pH 8.0, 1 mM EDTA followed by 500 ml 1 M NaCl 10 mM Tris–HCl pH 8.0, 1 mM EDTA and finally 10 mM Tris–HCl pH 8.0, 1 mM EDTA. The inclusion bodies were then solubilised in 20 mM Na phosphate, 30 mM Imidazole, 8 M Urea pH 7.4 and clarified by centrifugation before loading on a 5 ml HisTrap column (Pharmacia). The column was washed with 50 ml 20 mM Na phosphate, 30 mM Imidazole, 8 M Urea pH 7.4 and the purified $TrkAIg_2$ eluted with 25 ml 20 mM Na phosphate, 300 mM Imidazole, 8 M Urea pH 7.4.

The purified $TrkAIg_2$ protein was adjusted to a concentration of 0.1 mg/ml in 20 mM Na phosphate, 30 mM Imidazole, 8 M Urea pH 7.4, 1 mM β-mercaptoethanol and dialysed against 20 mM Tris–HCl, 50 mM NaCl, pH 8.5 (2 × 100 volumes). The dialysed protein was loaded onto a 1.6 ml Poros 20HQ column and eluted with a linear gradient of 0.025–1 M NaCl over 20 column volumes.

Competitive binding assay. Purified recombinant human NGF was radioiodinated with ^{125}I using a lactoperoxidase method and utilised in equilibrium binding studies with [I^{125}]-NGF as previously described (17). The binding assay used 0.23 nM [I^{125}]-NGF, unlabeled human NGF (concentration range: 10^{-6} M to 1×10^{-11} M), $TrkAIg_{1,2}$ (concentration range: 4×10^{-6} to 1×10^{-11} M), and $TrkAIg_2$ (concentration range 5×10^{-6} to 1×10^{-11} M) as previously described (15).

Surface plasmon resonance using BIACore. $TrkAIg_2$ was immobilised on a CM5 sensor chip by crosslinking the amine groups according to the manufacturer's instructions. NGF in the concentration range 1×10^{-9} to 5×10^{-6} M or BDNF at 1×10^{-6} M passed over at a flow rate of 20 μl/min. Data collected were analysed using BIAevaluation 3.0.

ELISA. The ELISA method has been described previously (18). Briefly, $TrkAIg_{1,2}$ in Coat I Buffer (50mM $NaHCO_3$, pH 9.6, 0.1% (w/v) NaN_3) was plated onto 96-well plates and incubated overnight at 4°C. Wells were emptied and 100μl Coat II (1% (w/v) BSA in Coat I) added to each well. After 2 h at 4°C, the plate was washed three times with Wash Buffer (50 mM Tris–HCl, pH 7.2, 200 mM NaCl, 0.1% (v/v) Triton X-100, 0.1% (w/v) NaN_3, 0.25% (w/v) gelatin). NGF (0–200 nM) was incubated at room temperature for 10 min with 2 mM $TrkAIg_2$ in Sample Buffer (1% BSA (w/v) in Wash Buffer) in a total volume of 50 μl. This was then added to the plate and incubated at room temperature for 1 h and washed as above. Anti-βNGF–β-galactosidase conjugate (Boehringer Mannheim) was then added (1:40, 50 μl per well), the plate incubated at RT for 2 h and washed as above. The assay was then developed by addition of 50 μl 200 mM 4-methyl umbelliferyl galactoside (4-MUG) in 100 mM Na phosphate, 1 mM $MgCl_2$, pH 7.3. After 20 min, the fluorescent product, 4-methylumbelliferone was measured using a fluorometer at excitation wavelength 364 nm, emission wavelength 448 nm.

TABLE I

Summary of Crystallographic Data Statistics for $TrkAIg_2$

	$TrkAIg_2$ data
Resolution range (Å, data collection)	40–1.9 (1.99–1.9)
Number of unique reflections	11 819
Redundancy	7.2 (5.7)
Completeness (%)	99.9 (99.7)
R_{merge} (%)	4.1 (23.3)
$I/\sigma(I)$	43.2 (4.4)
Refinement	
Resolution range (Å)	40–2.0 (2.09–2.0)
R_{cryst} (%)	23.7 (25.5)
R_{free} (%)	27.6 (28.9)
rsmd, bond lengths (Å)	0.016
rsmd, bond angles (°)	1.74
Number of non-hydrogen protein atoms	838
Number of solvent sites	34 (1 glycerol and 33 water molecules)
Average B value ($Å^2$)	
Main chain	44.1
Side chain	46.5
Solvent molecules	51.35

Circular dichroism. CD spectra were recorded at room temperature on a Jobin Yvon CD6 instrument using a cuvette of 0.5-mm path length at a protein concentration of 40 μM. Ten scans were accumulated with a scan speed of 0.5 nm/s. Spectra were averaged and the small signal arising from the buffer was subtracted.

Inhibition of neurite outgrowth of PC12 cells. Rat adrenal pheochromocytoma (PC12) cells were first cultured in DMEM supplemented with 5% fetal calf serum, 10% horse serum, 1% penicillin/streptomycin and 2 mM glutamine. Each dish contained 2×10^4 cells, 2 ng/ml human NGF and serial dilutions of $TrkAIg_2$ (concentration range: 2.5×10^{-6} to 1.56×10^{-7} M). Controls included wells without $TrkIg_2$ and also wells with and without NGF.

Inhibition of plasma extravasation. Plasma extravasation experiments used anaesthetised male Wistar rats (200–350 g) as previously described (15). For coinjection experiments, all skin sites received 100 μl (i.d.) of either NGF (8 pmol) or Tyrode (with or without $TrkA\text{-}Ig_{1,2}$ or $TrkIg_2$). For pretreatment experiments, skin sites received 100 μl (i.d.) of either $TrkA\text{-}Ig_{1,2}$ or $TrkAIg_2$ (24 or 80 pmol) or vehicle at −5 or −40 min. These sites then received 50 μl (i.d.) NGF (8 pmol) or Tyrode at start of accumulation period (0 min).

Structure determination. Expressed and purified protein was exchanged into 5 mM Bis-Tris buffer, pH 6.5, 0.1% sodium azide by ultrafiltration, and concentrated to 10 mg/ml. Initial crystallisation conditions were identified from commercially available screens (19). Refinement of these conditions produced diffraction quality crystals from a 1:1 mix of protein solution with 100–300 mM NaCl solution buffered with 100 mM Na citrate, pH 4.6–4.8.

Prior to data collection, crystals were cryoprotected by soaking in mother-liquor supplemented with glycerol. To maintain crystal viability, crystals were progressively soaked for 10 min in glycerol concentrations of 5, 10, 15, and 20% before being washed in 25% glycerol and immediately flash-frozen in a liquid nitrogen cold stream. X-ray data for these crystals were collected on station X11 at the EMBL-Hamburg outstation, DESY storage ring, to 1.9× at 100K. Data were processed with DENZO and scaled with SCALEPACK (20). A summary of data collection is presented in Table I.

The structure of $TrkAIg_2$ was solved by molecular replacement using AmoRe as implemented in CCP4 (21), and a monomer of the previously determined $P4_12_12$ form (with the swapped-strand deleted from the model (PDB:1WWA)). The structure was refined with CNS (22) (using data 40–2.0 Å at all stages), with iterative cycles of model building performed with O (23). 10% of the reflections were allocated for the R_{free} calculation (24). Six cycles of rebuilding and refinement lowered R_{cryst} and R_{free} to current values of 23.7 and 27.7%, respectively. A summary of refinement statistics is shown in Table I. The Ramachandran plot (25) as calculated with MOLEMAN2 reveals only 3 outliers, with 97% of non-glycyl residues lying in the core regions as described in Kleywegt and Jones (26).

RESULTS

Cloning and Expression of the Ig-like Domains, $TrkAIg_{1,2}$ and $TrkAIg_2$

Secondary structure analysis of the Ig-like regions using PredictProtein (16) showed defined stretches of β-strands. $TrkAIg_2$ has now been confirmed to adopt a fold similar to the I-set immunoglobulin domains, both in the work described here and by other studies. The first Ig-like domain, $TrkAIg_1$, comprises residues 160–252 in the mature extracellular domain of TrkA, while the second, $TrkAIg_2$ consists of residues 253–349. An alternatively spliced form of TrkA, containing a six amino acid insert in the proline rich domain (C-terminal to $TrkAIg_2$), VSFSPV, shows a higher affinity for NT3 and therefore may be important for neurotrophin binding (27). This sequence is also found in rat TrkA and a similar sequence is found in the chicken TrkA. There is also an insert of polar residues in all of the TrkB sequences (28). It is likely that this proline rich region may contribute to ligand binding and/or specificity and was therefore included in the $TrkAIg_{1,2}$ and $TrkAIg_2$ constructs. The DNA encoding the second Ig-like domain was amplified by PCR and ligated into the T7 expression vector pET15b (Novagen). After induction the protein was found to be expressed in inclusion bodies as with $TrkAIg_{1,2}$ (15). The Trk proteins were refolded by dialysis to remove the denaturant and reducing reagent. Subsequently, the different folded states were resolved by ion exchange chromatography (Fig. 1A). $TrkAIg_2$ elutes in three peaks and SDS–PAGE revealed that all three were of the expected molecular weight. The most likely explanation is that the refolding resulted in different conformations.

NGF Binding Properties of the Ig-like Domains

To determine which of the protein fractions eluting from the Poros 20HQ column contained NGF binding activity, two methods were used: an ELISA and a competitive binding assay. For the ELISA, $TrkAIg_{1,2}$ was plated on a 96-well plate to which different concentrations of NGF, pre-incubated with $TrkAIg_2$, were added. An anti-NGF β-galactosidase conjugate was then added and the fluorescence measured after addition of substrate (Fig. 2A). The competitive binding assay makes use of A875 cells (29), which express only the $p75^{NGFR}$ receptor, to bind $[I^{125}]$-NGF. The competing TrkAIg domains were incubated with the cells and the

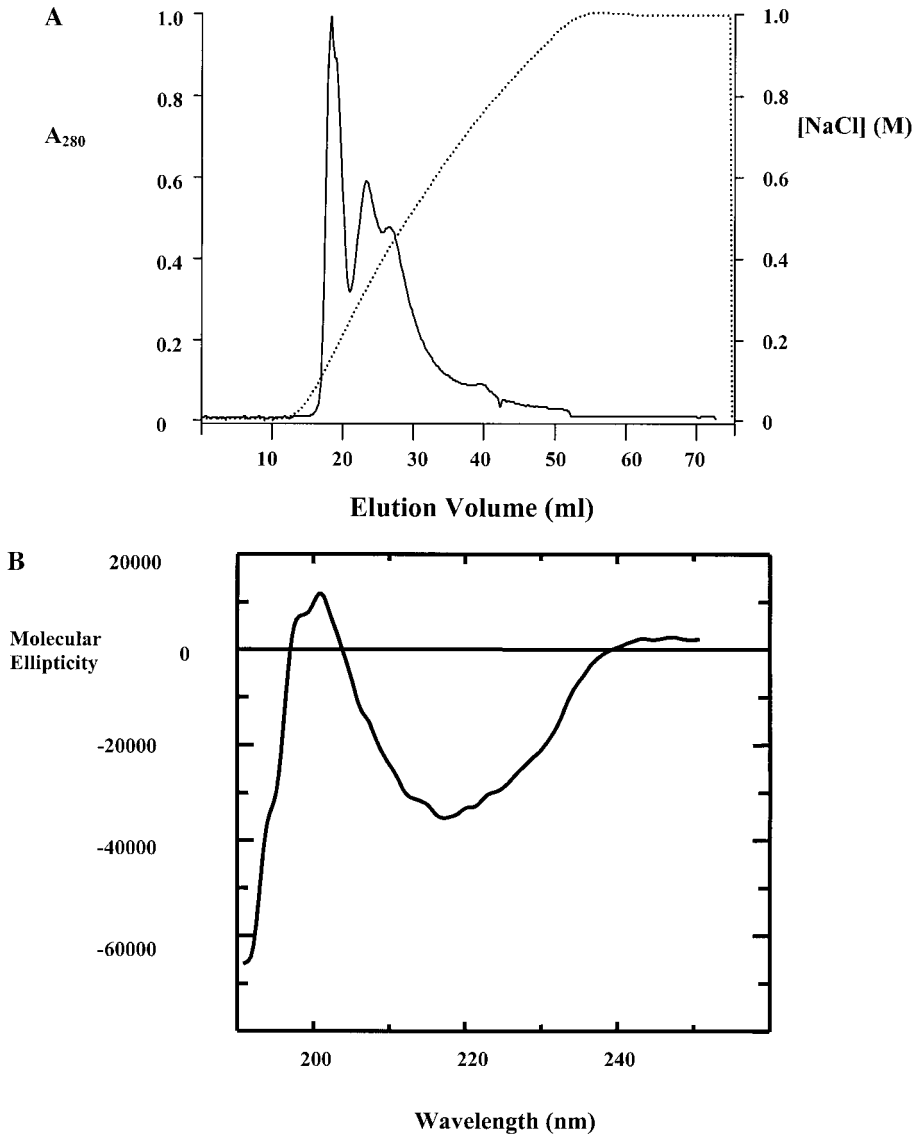

FIG. 1. (A) Elution profile of $TrkAIg_2$ (solid line) using ion exchange chromatography (Poros 20HQ) with a linear gradient of 0.025–1 M NaCl (dotted line). (B) Circular dichroism spectrum of $TrkAIg_2$. The molecular ellipticity (theta) as a function of wavelength.

amount of cell-bound NGF was determined. The first peak eluting from the Poros 20HQ column for $TrkAIg_2$ was the only one to bind NGF in the competitive binding assay. Circular dichroism (Fig. 1B) of the active $TrkAIg_2$ shows a minimum at 218 nm and a maximum near 200 nm. This is typical of anti-parallel β-sheet structures, which display a negative Cotton effect with a minimum near 218 nm and a positive effect with a maximum at around 195 nm (30). Similar results have been reported for other immunoglobulin domains (31) and for $TrkAIg_{1,2}$ (15). The $TrkAIg_2$ showed a 40% reduction in fluorescence by ELISA at 200 nM NGF. Similar results were obtained by the competitive binding (data not shown). Thus it seemed likely that the $TrkAIg_2$ was responsible for the NGF binding attributed to $TrkAIg_{1,2}$ (15). Receptor binding with A875 cells shows that there is a threefold difference in the IC_{50} for $TrkAIg_2$ binding to NGF compared to $TrkAIg_{1,2}$ (Fig. 2B). This results in a K_D for this interaction of 9.9 nM. The K_D for the interaction between $TrkAIg_{1,2}$ and NGF has previously been shown to be 3.3 nM (15). Data from surface plasmon resonance indicate that the expressed $TrkAIg_2$ binds NGF with a K_D of 11.8 nM (R_{max} = 309, $k_d(1/s) = 8.66 \times 10^{-4}$; $k_a(1/Ms) = 7.32 \times 10^4$) which is in agreement with the K_D of 9.9 nM from the competitive binding data. Since the K_D of ectopically expressed TrkA binding to NGF in mammalian cells was shown to be between 0.1 and 1.0 nM (32, 33) our results indicate that the major contributor to NGF binding is to be found within $TrkAIg_2$. In addition, we found that BDNF at 1 μM did not bind to $TrkAIg_2$ (data not shown), indicating that $TrkAIg_2$ is specific for NGF.

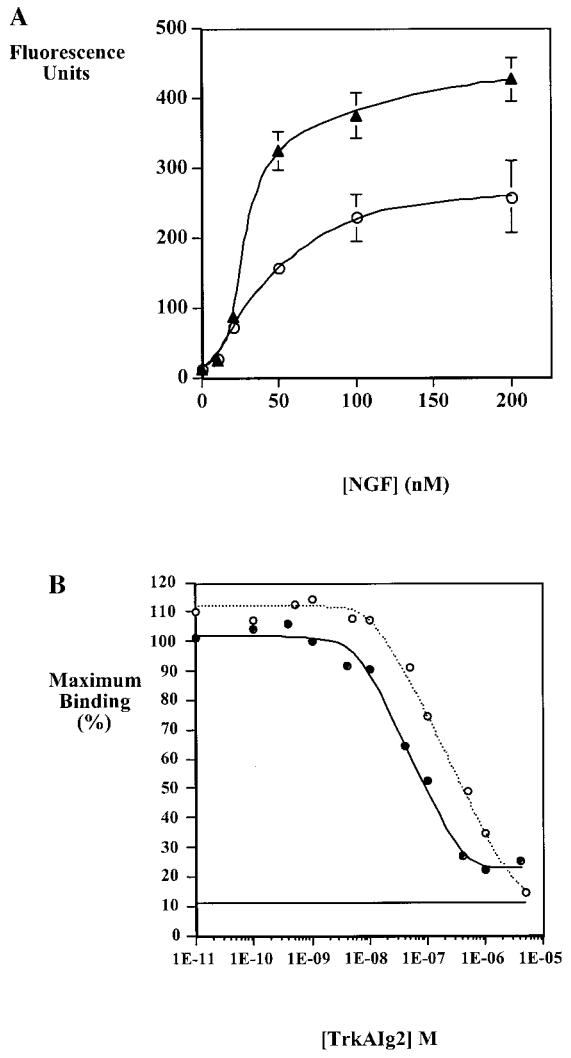

FIG. 2. NGF binding properties of the Ig-like domains: (A) Binding of NGF to $TrkAIg_{1,2}$ in ELISA competition with NGF alone (triangles), or $TrkAIg_2$ (open circles). (B) Receptor binding assay with A875 cells. Inhibition of [^{125}I]-NGF binding by $TrkAIg_{1,2}$ (closed circles) and $TrkAIg_2$ (open circles). Complete displacement by 1 μM cold NGF indicated as straight line.

Crystal Structure of $TrkIg_2$

The $TrkAIg_2$ construct used in this study crystallised in space group $P4_322$, with a single molecule in the asymmetric unit. The final model described here spans residues 285 to 388 of the $TrkAIg_2$ sequence, with the first three residues at the N-terminus (labelled 282–284 in the model) derived from the uncleaved histidine-tag sequence of the expressed construct. A schematic representation of the monomer is shown in Fig. 3. Twenty-five additional residues present on the C-terminus in the prepared construct were not observed in the electron density. The model contains 34 solvent molecules (1 glycerol, and 33 water molecules).

In this new crystal form, $TrkAIg_2$ adopts the same I-set immunoglobulin domain topology previously described for the $P4_12_12$ structure. In both cases the protein forms a strand-swapped dimer, with the NH_2-terminal A strand of each molecule forming part of the fold of the adjacent monomer (Fig. 3). In the $P4_322$ crystals there is a single monomer in the asymmetric unit, with the dimer being generated by one of the 2-fold crystallographic axes. The $P4_322$ monomer overlays on each of the two monomers of the $P4_12_12$ form with a root mean square (rms) deviation of 0.75 and 0.6 Å, respectively (based on the 95 equivalent Cα positions of residues 285–379). Similarly, the arrangement of the respective dimers is comparable, with an overall rms deviation of 0.79 Å (based on a simultaneous overlay of residues 285–379 from each monomer of the two dimers). This overlay is illustrated in Fig. 3.

As described previously for the $P4_12_12$ crystal form, in the $P4_322$ crystals the TrkAIg2 domain consists of two beta sheets, formed from strands ABED and CFG, respectively. In each monomer the A strand is contributed from the adjacent polypeptide chain, with residues 295–297 forming a short crossover region between the two domains of the dimer. There is a single disulphide bond in each domain (Cys 300—Cys 345), exposed on the protein surface and linking the B and E strands from the same sheet. An overlay of the $P4_12_12$ and $P4_322$ crystal structures (Fig. 3) shows there is a single region in which the two structures differ significantly—residues 378 to 386 at the carboxy-terminus where the chain exits and extends away from the confines of the Ig-domain. The construct used in this study includes residues from the proline-rich region which connects the Ig domains to the membrane, and as mentioned above, most of these residues are disordered within the crystal lattice. Localised crystal contacts most likely give rise to the differing conformations of this region in the two crystal structures. The observed conformations of these regions in the two crystal lattices may not reflect biologically relevant forms in the intact receptor.

This further structure of a truncated form of TrkA confirms the propensity of the $TrkAIg_2$ domain to form strand-swapped homodimers. $TrkAIg_2$ is unable to bind neurotrophins in this form as the face that makes contact with NGF in the crystal structure of the $TrkAIg_2$:NGF complex is buried within the dimer. Also, the conformation of the A–B turn and the A-strand in homodimeric $TrkAIg_2$ are not consistent with the formation of an $TrkAIg_2$:NGF complex (illustrated in Fig. 4). Nonetheless, the recombinant form of $TrkAIg_2$ used in this study was specifically isolated using gel-filtration, after refolding, as a monomer. The aggregation state has been further examined using ultracentrifugation which confirms this species exists in equilibrium as a mixture of monomers and dimers (data not shown). The protein is active in binding studies, an indication of a monomeric state. In total, these data do not suggest dimerisation is an artefact of the

re-folding process used to solubilise the recombinant protein from inclusion bodies. It seems more likely that interactions between the A-strand and the remainder of the isolated domain are inherently weak, such that at the high protein concentrations used for crystallisation a strand-swapped dimer is energetically more stable than two monomers. In addition to the extensive interchain contacts provided through the strand swapping, dimerisation buries 1018 $Å^2$ of surface area between the two domains. The majority of this surface area is provided by hydrophobic groups (719 $Å^2$, as calculated in QUANTA) implying an entropic advantage for dimer formation. Crystal structures of metastable, strand-swapped forms of the NH_2-terminal domain of CD2 have previously been described (34) and concentration-dependent transitions between intertwined forms of CD2 have also been demonstrated (35). The CD2 NH_2-terminal domain and $TrkAIg_2$ are both single immunoglobulin superfamily domains derived from multidomain receptors but expressed in isolation. It is unclear whether this mode of oligomerisation can take place in the respective intact receptors, where neighbouring domains may limit transitions of this type. Both studies illustrate a potential limitation in the exploitation of recombinantly truncated protein products for functional studies.

Inhibition of NGF-Induced Neurite Outgrowth in Vitro

PC12 cells express both $p75^{NGFR}$ and TrkA and differentiate in the presence of NGF, displaying a neuronal phenotype forming neurites (36). Addition of $TrkAIg_2$ shows inhibition of NGF-induced neurite outgrowth, suggesting that $TrkAIg_2$ sequesters NGF, thus preventing its binding to the cellular receptors (Fig. 5).

Inhibition of NGF Induced Plasma Extravasation in Vivo

Intradermal injection of NGF stimulates plasma extravasation, causing oedema formation (37, 38). We have previously shown that $TrkAIg_{1,2}$ can inhibit NGF-induced plasma extravasation *in vivo* (15); here we examined the ability of $TrkAIg_2$ to do the same (Fig. 6). When mixed and co-injected with 8 pmol NGF, 24 pmol $TrkAIg_{1,2}$ and 80 pmol $TrkAIg_2$ antagonise the effect of NGF ($P = 0.01$, $n = 6$ and $P < 0.001$, $n = 4–8$ respectively as assessed by ANOVA with Bonferroni's post-test when compared to sites receiving NGF alone) (Figs. 6A and 6B). To investigate the ability of $TrkAIg_{1,2}$ and $TrkAIg_2$ to antagonise NGF *in vivo,* skin sites were pre-treated by intradermal injection of either $TrkAIg_{1,2}$, or $TrkAIg_2$. NGF was given (i.d.) 5 or 40 min later. Pre-treatment of the site with $TrkAIg_{1,2}$ and $TrkAIg_2$ showed that after 5 min, 24 pmol $TrkAIg_{1,2}$ and 80 pmol $TrkAIg_2$ were still able to antagonise NGF. After 40 min both $TrkAIg_{1,2}$ and $TrkAIg_2$ still had a significant effect only at 80 pmol ($P < 0.05$, $n = 4$ and $P < 0.001$, $n = 3$) (Figs. 6C–6F). Neither of the TrkAIg proteins induced plasma extravasation when injected alone at any doses used. Both proteins failed to inhibit plasma extravasation induced by the neurokinin NK_1 agonist GR73632, a NGF-independent mediator of oedema formation. These results clearly indicate that $TrkAIg_2$ can act selectively to bind to and inhibit the biological action of NGF *in vivo.*

DISCUSSION

The loss of cholinergic function in the basal forebrain, associated with memory loss, is one of the earliest changes in Alzheimer's disease. NGF is a potent neurotrophic factor for forebrain cholinergic neurones and promotes the survival and differentiation of sympathetic and sensory neurones during development (39, 40). In animal models it has been shown that administration of NGF corrects the effects of cholinergic atrophy in aged (41) or lesioned animals (42–47). The success with animal studies prompted similar studies with patients suffering from Alzheimer's disease (48, 49). Administration of purified mouse NGF resulted in increased cerebral blood flow, reduced slow-wave EEG activity and nicotinic cholinergic receptor density and although clear cognitive amelioration could not be shown, slight improvements in the results of neuropsychological tests were observed. This treatment, however, requires expensive, invasive surgery, as NGF cannot cross the blood-brain barrier. This will limit the number of sufferers who could be treated and therefore a long-term solution would be the generation of small molecule agonists able to mimic the trophic actions of NGF.

Structure-based drug design of small molecule agonists of NGF relies on knowledge of the interaction of NGF with the receptor, TrkA, whereas the random screening approach requires a target molecule. It is therefore essential to identify the domain of TrkA responsible for NGF binding and receptor activation.

Several studies have attempted to define such domain(s). Thus, a fusion protein consisting of maltose binding protein and the second LRM of TrkA has been shown to bind NGF with a similar affinity to the entire extracellular domain of TrkA, and a peptide corresponding to the second LRM of TrkA blocked NGF binding to TrkA (10, 11). The second LRM of TrkB has been shown to bind BDNF, NT3 and NT4/5 but not NGF (11, 12). Naturally occurring TrkB variants lacking two or all three LRMs do not bind BDNF, NT3 or NT4/5 (50). However, further analysis of the role of LRMs in neurotrophin binding revealed that deletion of the LRMs from TrkA does not abolish TrkA autophosphorylation but does change the differentiative

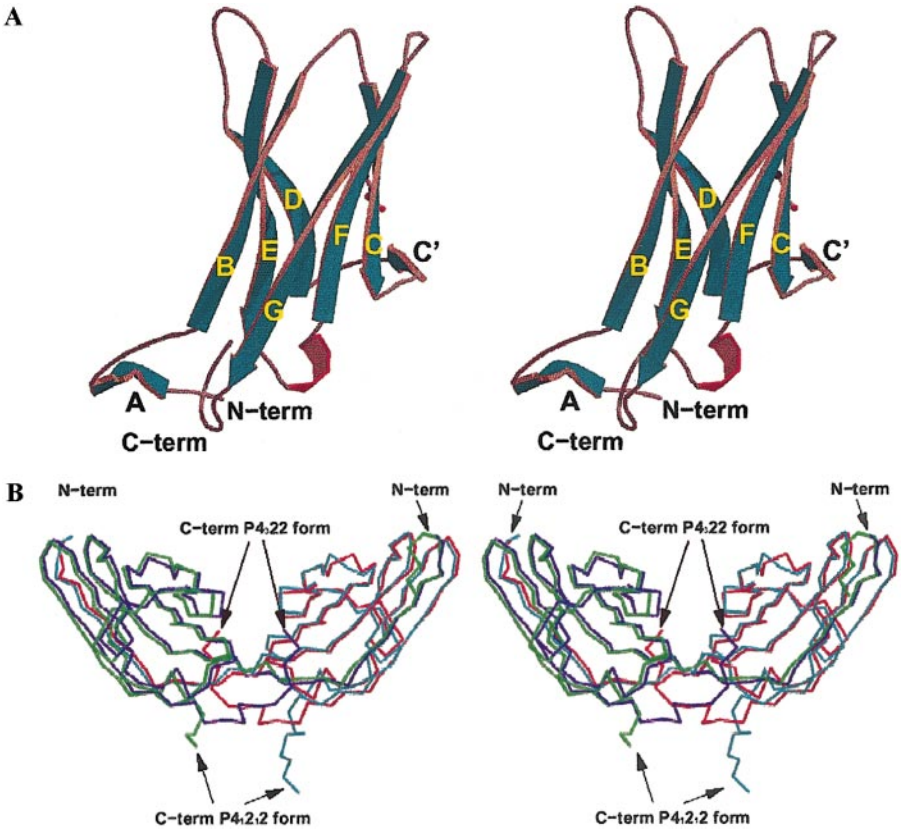

FIG. 3. (A) Schematic representation of the $TrkAIg_2$ monomer, with the beta-sheets that make up the Immunoglobulin fold labelled. (B) Overlay of the dimeric forms of $TrkAIg_2$. In green/cyan is the previously determined $P4_12_12$ crystal form, and in blue/red is the $P4_322$ form described here. Figure prepared with MOLSCRIPT (52) and RASTER3D (53).

phenotype in neurotrophin responsive cells, resulting in loss of the high affinity NT3 but not NGF binding (51).

Other evidence suggests that binding of the neurotrophins to their high affinity Trk receptors is mediated predominantly through interaction with the Ig-like domains. Transiently transfected cells expressing chimeric proteins, in which both Ig-like domains of TrkB were replaced with those of TrkA, are able to bind NGF with the same affinity as cells expressing wild type TrkA (13). Similar results were obtained by replacing the same domains in TrkC with those of

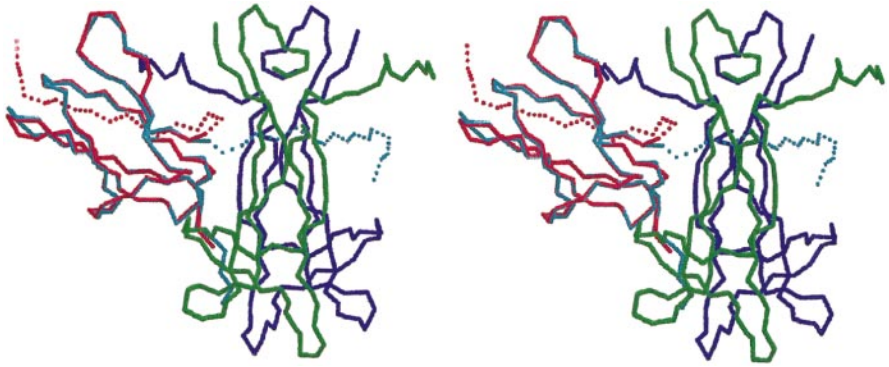

FIG. 4. Cα-trace stereoview of the $TrkAIg_2$:NGF complex (NGF monomers in green/blue, $TrkAIg_2$ monomer in red). The second $TrkAIg_2$ monomer is omitted for clarity. Shown overlaid on the $TrkAIg_2$ monomer are the coordinates of one half of the $TrkAIg_2$ strand-swapped dimer (cyan). Residues from the "swapped-strand" are shown as dots in both $TrkAIg_2$ structures. Both the position of the swapped strand and the conformation of the A–B turn in the homodimeric $TrkAIg_2$ form are not consistent with NGF binding. Figure prepared with MOLSCRIPT (52) and RASTER3D (53).

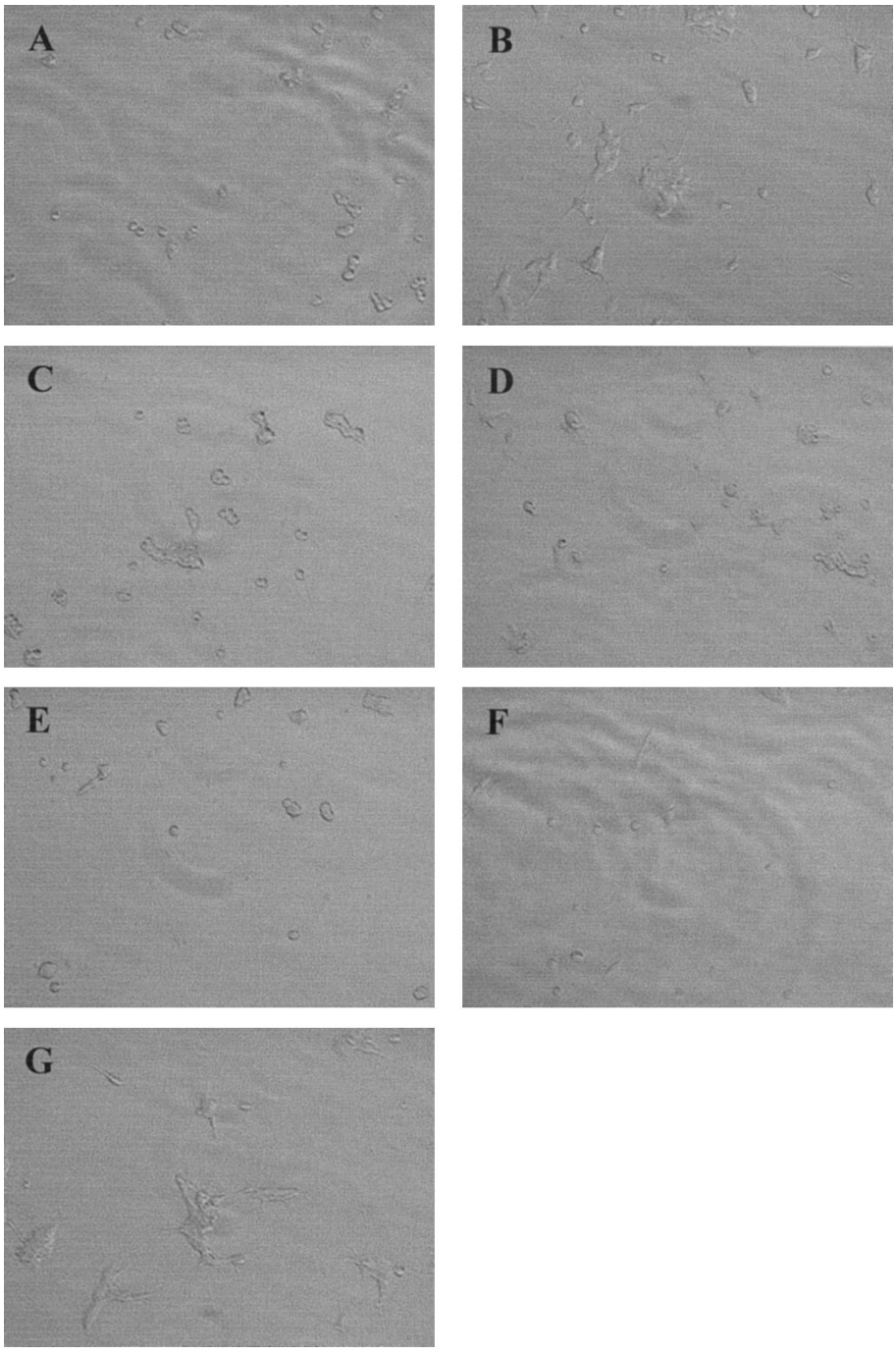

FIG. 5. PC12 cells neurite outgrowth assay. (A) Untreated PC12 cells. (B) PC12 cells grown in the presence of 2 ng/ml NGF. (C–F) PC12 cells grown in the presence of 2 ng/ml NGF and $TrkAIg_2$ at 5 μM (C), 1.25 μM (D), 0.325 μM (E), 0.039 μM (F), and 0.009 μM (G).

TrkA (14). Furthermore, this group showed that expression of truncated TrkA and TrkC receptors, consisting of only the second Ig-like domain and tyrosine kinase domain, was sufficient for specific neurotrophin binding and for phosphorylation of the truncated TrkC by NT3.

Recently the structure of NGF bound to the $TrkAIg_2$ domain has been elucidated (9). The structures of $TrkAIg_2$, $TrkBIg_2$ and $TrkCIg_2$ have been published (8) and all form strand-swapped dimers. These proteins were therefore biologically inactive. For the co-crystallisation study (9) $TrkAIg_{1,2}$ was mixed with NGF and the subsequent crystals revealed that $TrkAIg_1$ domain had been proteolysed away leaving only the $TrkAIg_2$ domain bound to NGF. This data did not therefore show definitively that $TrkAIg_2$ on its own

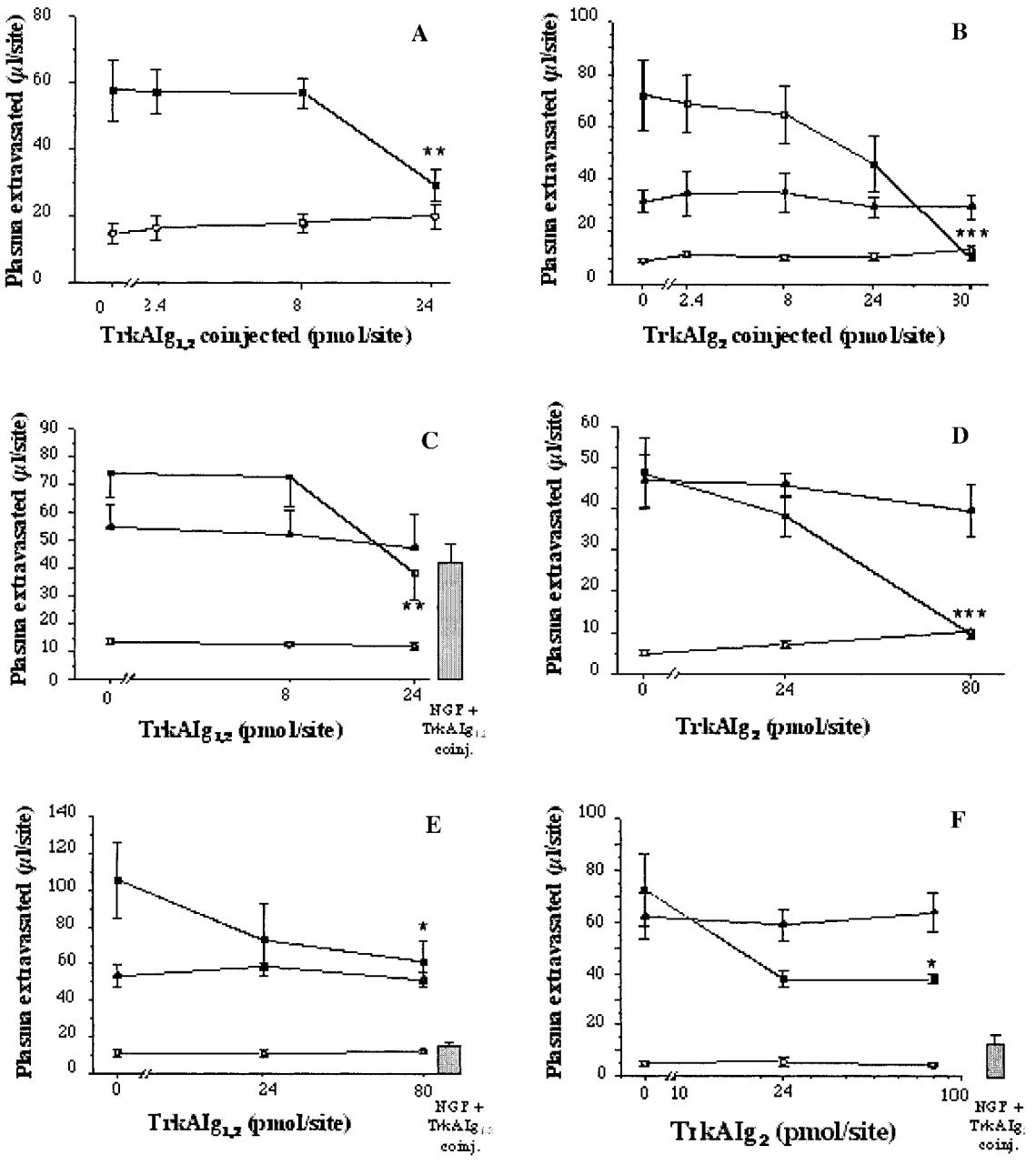

FIG. 6. Plasma extravasation with NGF injected. Inhibition of plasma extravasation with increasing concentration of $TrkAIg_{1,2}$. (A) or $TrkAIg_2$ (B). Inhibition of plasma extravasation with 5 min pretreatment with $TrkAIg_{1,2}$ (C) and $TrkAIg_2$ (D). Inhibition of plasma extravasation with 40 min. pretreatment with $TrkAIg_{1,2}$ (E) and $TrkAIg_2$ (F). Vehicle (open circle), GR73632, 30 pmol (triangle). (A, C, and E) $TrkAIg_{1,2}$ (closed square) (B, D, and F) $TrkAIg_2$ (closed square). For comparison, the response induced by 8 pmol 7S NGF coinjected with 24 pmol $TrkAIg_{1,2}$ (C and E) and with 24 pmol $TrkAIg_2$ (F) is shown by the filled bar.

can bind to NGF. We have previously shown that the Ig-like domains of TrkA, expressed as recombinant protein can bind NGF with a similar affinity to that of the native receptor, expressed on the cell surface (15). The data we present here shows conclusively that $TrkAIg_2$ binds NGF with an affinity similar to that of the entire extracellular domain. We have produced $TrkAIg_2$ as a recombinant protein and have determined its structure, confirming it as an I-type immunoglobulin domain that forms a strand-swapped homodimer under the crystallisation conditions used. Although it remains unclear whether strand-swapping can occur in the intact TrkA extracellular domains, if this was the case dimerisation could act as a molecular switch regulating the binding activity of the receptor. Using a combination of the results from these binding studies and the crystal structures of the $TrkAIg_2$ domains available, we aim to utilise $TrkAIg_2$ as a target

for high throughput assays for the isolation of small molecule NGF analogues.

ACKNOWLEDGMENTS

A.G.S.R. and S.J.A. are Sigmund Gestetner fellows, A.R.C. is a Lister Institute Research Fellow, and G.S.B. holds a British Heart Foundation Ph.D. studentship. We thank Enact Pharma PLC, the Wellcome Trust and BRACE (Bristol Research into Care of the Elderly) for their support. We also thank the staff of the EMBL-Hamburg outstation for their expert help with X-ray data collection. Some of the work reported here is the subject of patent application No. 9807781.1. The coordinates and structure factors for the $TrkAIg_2$ domain have been deposited with the Protein Data Bank, with Accession Codes 1HE7 and R1HE7SF.

REFERENCES

1. Rodriguez-Tebar, A., Dechant, G., Gotz, R., and Barde, Y. A. (1992) Binding of neurotrophin-3 to its neuronal receptors and interactions with nerve growth-factor and brain-derived neurotrophic factor. *EMBO J.* **11,** 917–922.
2. Martin-Zanca, D., Oskam, R., Mitra, G., Copeland, T., and Barbacid, M. (1989). Molecular and biochemical-characterization of the human trk proto-oncogene. *Mol. Cell. Biol.* **9,** 24–33.
3. Ip, N. Y., Stitt, T. N., Tapley, P., Klein, R., Glass, D. J., Fandl, J., Greene, L. A., Barbacid, M., and Yancopoulos, G. D. (1993) Similarities and differences in the way neurotrophins interact with the trk receptors in neuronal and nonneuronal cells. *Neuron* **10,** 137–149.
4. Klein, R., Lamballe, F., Bryant, S., and Barbacid, M. (1992) The trkB tyrosine protein-kinase is a receptor for neurotrophin-4. *Neuron* **8,** 947–956.
5. Lamballe, F., Klein, R., and Barbacid, M. (1991) TrkC, a new member of the trk family of tyrosine protein-kinases, is a receptor for neurotrophin-3. *Cell* **66,** 967–979.
6. Urfer, R., Tsoulfas, P., Soppet, D., Escandon, E., Parada, L. F., and Presta, L. G. (1994) The binding epitopes of neurotrophin-3 to its receptors trkc and gp75 and the design of a multifunctional human neurotrophin. *EMBO J.* **13,** 5896–5909.
7. Schneider, R., and Schweiger, M. (1991) A novel modular mosaic of cell-adhesion motifs in the extracellular domains of the neurogenic trk and trkb tyrosine kinase receptors. *Oncogene* **6,** 1807–1811.
8. Ultsch, M. H., Wiesmann, C., Simmons, L. C., Henrich, J., Yang, M., Reilly, D., Bass, S. H., and deVos, A. M. (1999). Crystal structures of the neurotrophin-binding domain of TrkA, TrkB and TrkC. *J. Mol. Biol.* **290,** 149–159.
9. Wiesmann, C., Ultsch, M. H., Bass, S. H., and deVos, A. M. (1999) Crystal structure of nerve growth factor in complex with the ligand- binding domain of the TrkA receptor. *Nature* **401,** 184–188.
10. Windisch, J. M., Marksteiner, R., and Schneider, R. (1995) Nerve growth-factor binding-site on trka mapped to a single 24-amino acid leucine-rich motif. *J. Biol. Chem.* **270,** 28133–28138.
11. Windisch, J. M., Auer, B., Marksteiner, R., Lang, M. E., and Schneider, R. (1995) Specific neurotrophin binding to leucine-rich motif peptides of trka and trkb. *FEBS Lett.* **374,** 125–129.
12. Windisch, J. M., Marksteiner, R., Lang, M. E., Auer, B., and Schneider, R. (1995) Brain-derived neurotrophic factor, neurotrophin-3, and neurotrophin-4 bind to a single leucine-rich motif of trkb. *Biochemistry* **3,** 11256–11263.
13. Perez, P., Coll, P. M., Hempstead, B. L., Martinzanca, D., and Chao, M. V. (1995) NGF binding to the trk tyrosine kinase receptor requires the extracellular immunoglobulin-like domains. *Mol. Cell. Neurosci.* **6,** 97–105.
14. Urfer, R., Tsoulfas, P., O'Connell, L., Shelton, D. L., Parada, L. F., and Presta, L. G. (1995) An immunoglobulin-like domain determines the specificity of neurotrophin receptors. *EMBO J.* **14,** 2795–2805.
15. Holden, P. H., Asopa, V., Robertson, A. G. S., Clarke, A. R., Tyler, S., Bennett, G. S., Brain, S. D., Wilcock, G. K., Allen, S. J., Smith, S., and Dawbarn, D. (1997) Immunoglobulin-like domains define the nerve growth factor binding site of the TrkA receptor. *Nat. Biotechnol.* **15,** 668–672.
16. Rost B., and Sander C. (1993) Prediction of protein secondary structure at better than 70-percent accuracy. *J. Mol. Biol.* **232,** 584–599.
17. Treanor, J. J. S., Dawbarn, D., Allen, S. J., Macgowan, S. H., and Wilcock, G. K. (1991) Low affinity nerve growth-factor receptor-binding in normal and Alzheimer's disease basal forebrain. *Neurosci. Lett.* **121,** 73–76.
18. Allen, S. J., MacGowan, S. H., Treanor, J. J. S., Feeney, R., Wilcock, G. K., and Dawbarn, D. (1991) Normal NGF content in Alzheimer's disease cerebral cortex and hippocampus. *Neurosci. Lett.* **131,** 135–139.
19. Jancarik, J., and Kim, S. H. (1991) Sparse-matrix sampling—A screening method for crystallisations of proteins. *J. Appl. Crystallogr.* **24,** 409–411.
20. Otwinowski, Z., and Minor, W. (1996) Processing of X-ray diffraction data collected in oscillation mode. *Methods Enzymol.* **276,** 307–326.
21. 4 CCPN. The CCP4 Suite: Programs for Protein Crystallography (1994) *Acta Crystallogr. Sect. D* **50,** 760–763.
22. Brünger, A. T., Adams, P. D., Clore, G. M., DeLano, W. L., Gros, P, Grosse-Kunstleve, R. W., Jiang, J-S., Kuszewski, J., Nilges, M., Pannu, N. S., Read, R. J., Rice, L. M., Simonson, T., and Warren, G. L. (1998) Crystallography & NMR system: A new software suite for macromolecular structure determination. *Acta Crystallogr. Sect. D* **54,** 905–921.
23. Jones, T. A., Zou, J-Y., Cowan, S. W., and Kjeldgaard, M. (1991) Improved methods for building protein structures in electron-density maps and the location of errors in these models. *Acta Crystallog. Sect. A* **47,** 110–119.
24. Brünger, A. T. (1992) The free *R* value: A novel statistical quantity for assessing the accuracy of crystal structures. *Nature* **355,** 472–474.
25. Ramachandran, G. N., and Sasisekharan, V. (1968) Conformation of polypeptides and proteins. *Adv. Protein Chem.* **23,** 283–437.
26. Kleywegt, G. J., and Jones, T. A. (1996) Phi/psi-chology: Ramachandran revisited. *Structure* **4,** 1395–1400.
27. Clary, D. O., and Reichardt, L. F. (1994) An alternatively spliced form of the nerve growth-factor receptor trka confers an enhanced response to neurotrophin-3. *Proc. Natl. Acad. Sci. USA* **91,** 11133–11137.
28. Allen, S. J., Dawbarn, D., Eckford, S. D., Wilcock, G. K., Ashcroft, M., Colebrook, S. M., Feeney, R., and Macgowan, S. H. (1994) Cloning of a noncatalytic form of human trkb and distribution of messenger-RNA for trkb in human brain. *Neuroscience* **60,** 825–834.
29. Vale, R. D., and Shooter, E. M. (1985) Assaying binding of nerve growth-factor to cell-surface receptors. *Methods Enzymol.* **109,** 21–39.
30. Yang, J. T., Wu, C. S. C., and Martinez, H. M. (1986) Calculation of protein conformation from circular-dichroism. *Methods Enzymol.* **130,** 208–269.
31. Ikeda, K., Hamaguchi, K., and Migita, S. (1968) Circular dichro-

ism of Bence–Jones proteins and immunoglobulins. *J. Biochem.* **63,** 654–660.

32. Kaplan, D. R., Hempstead, B. L., Martinzanca, D., Chao, M. V., and Parada, L. F. (1991) The trk protooncogene product—A signal transducing receptor for nerve growth-factor. *Science* **252,** 554–558.
33. Loeb, D. M., Maragos, J., Martinzanca, D., Chao, M. V., Parada, L. F., and Greene, L. A. (1991) The trk protooncogene rescues NGF responsiveness in mutant NGF-nonresponsive pc12 cell-lines. *Cell* **66,** 961–966.
34. Murray, A. J., Head, J. G., Barker, J. J., and Brady, R. L. (1998) Engineering an intertwined form of CD2 for stability and assembly. *Nat. Struct. Biol.* **5,** 778–782.
35. Hayes M. V., Sessions R. B., Brady R. L., and Clarke A. R. (1999) Engineered assembly of intertwined oligomers of an immunoglobulin chain. *J. Mol. Biol.* **285,** 1857–1867.
36. Fujimori, K., Fukuzono, S., Kotomura, N., Kuno, N., and Shimizu, N. (1992) Overproduction of biologically-active human nerve growth-factor in *Escherichia-coli. Biosci. Biotechnol. Biochem.* **56,** 1985–1990.
37. Bennett, G. S., and Brain, S. D. (1996) Nerve growth factor induces an immediate and also a late phase of oedema formation in rat skin. *Br. J. Pharmacol.* **119,** P55.
38. Otten, U., Baumann, J. B., and Girard, J. (1984) Nerve growth-factor induces plasma extravasation in rat skin. *Eur. J. Pharmacol.* **106,** 199–201.
39. Thoenen, H., Bandtlow, C., and Heumann, R. (1987) The physiological-function of nerve growth-factor in the central-nervous-system—Comparison with the periphery. *Rev. Physiol. Biochem. Pharmacol.* **109,** 145–178.
40. Hatanaka, H., Tsukui, H., and Nihonmatsu, I. (1988) Developmental-change in the nerve growth-factor action from induction of choline-acetyltransferase to promotion of cell-survival in cultured basal forebrain cholinergic neurons from postnatal rats. *Dev. Brain Res.* **39,** 85–95.
41. Fischer, W., Wictorin, K., Bjorklund, A., Williams, L. R., Varon, S., and Gage, F. H. (1987) Amelioration of cholinergic neuron atrophy and spatial memory impairment in aged rats by nerve growth-factor. *Nature* **329,** 65–68.
42. Tuszynski M. H., U H. S., Amaral D. G., and Gage F. H. (1990) Nerve growth-factor infusion in the primate brain reduces lesion-induced cholinergic neuronal degeneration. *J. Neurosci.* **10,** 3604–3614.
43. Junard, E. O., Montero, C. N., and Hefti, F. (1990) Long-term administration of mouse nerve growth-factor to adult-rats with partial lesions of the cholinergic septohippocampal pathway. *Exp. Neurol.* **110,** 25–38.
44. Kromer, L. F. (1987) Nerve growth-factor treatment after brain injury prevents neuronal death. *Science* **235,** 214–216.
45. Hefti F. (1986). Nerve growth-factor promotes survival of septal cholinergic neurons after fimbrial transections. *J. Neurosci.* **6,** 2155–2162.
46. Montero, C. N., and Hefti, F. (1988) Rescue of lesioned septal cholinergic neurons by nerve growth-factor—Specificity and requirement for chronic treatment. *J. Neurosci.* **8,** 2986–2999.
47. Montero, C. N., and Hefti, F. (1989) Intraventricular nerve growth-factor administration prevents lesion-induced loss of septal cholinergic neurons in aging rats. *Neurobiol. Aging* **10,** 739–743.
48. Olson, L., Nordberg, A., Vonholst, H., Backman, L., Ebendal, T., Alafuzoff, I., Amberla, K., Hartvig, P., Herlitz, A., Lilja, A., Lundqvist, H., Langstrom, B., Meyerson, B., Persson, A., Viitanen, M., Winblad, B., and Seiger, A. (1992) Nerve growth-factor affects c-11 nicotine binding, blood-flow, eeg, and verbal episodic memory in an alzheimer patient. *J. Neural Transm. Parkinsons Dis. Dementia Sect.* **4,** 79–95.
49. Jonhagen, M. E., Nordberg, A., Amberla, K., Backman, L., Ebendal, T., Meyerson, B., Olson, L., Seiger, A., Shigeta, M., Theodorsson, E., Viitanen, M., Winblad, B., and Wahlund, L. O. (1998) Intracerebroventricular infusion of nerve growth factor in three patients with Alzheimer's disease. *Dementia Geriatr. Cogn. Disorders* **9,** 246–257.
50. Ninkina, N., Grashchuck, M., Buchman, V. L., and Davies, A. M. (1997) TrkB variants with deletions in the leucine-rich motifs of the extracellular domain. *J. Biol. Chem.* **272,** 13019–13025.
51. MacDonald, J. I. S., and Meakin, S. O. (1996) Deletions in the extracellular domain of rat trkA lead to an altered differentiative phenotype in neurotrophin responsive cells. *Mol. Cell. Neurosci.* **7,** 371–390.
52. Kraulis, P. J. (1991) MOLSCRIPT: A program to produce both detailed and schematic plots of protein structures. *J. App. Crystallog.* **24,** 946–950.
53. Meritt, E. A., and Bacon, D. J. (1997) Raster3D photorealistic molecular graphics. *Methods Enzymol.* **277,** 505–524.